ELSEVIER

Cardiovascular Research 42 (1999) 530–542

Cardiovascular Research

Pause induced early afterdepolarizations in the long QT syndrome: a simulation study

Prakash C. Viswanathan[a], Yoram Rudy[b,*]

[a]*Department of Physiology and Biophysics, Cardiac Bioelectricity Research and Training Center, Case Western Reserve University, Cleveland, OH 44106-7207, USA*

[b]*Department of Biomedical Engineering, Cardiac Bioelectricity Research and Training Center, 505 Wickenden Building, Case Western Reserve University, Cleveland, OH 44106-7207, USA*

Received 14 October 1998; accepted 4 January 1999

Abstract

Objective: The long QT syndrome (LQTS) is characterized by prolonged repolarization and propensity to syncope and sudden death due to polymorphic ventricular tachycardias such as torsade de pointes (TdP). The exact mechanism of TdP is unclear, but pause-induced early afterdepolarizations (EADs) have been implicated in its initiation. In this study we investigate the mechanism of pause-induced EADs following pacing at clinically relevant rates and characterize the sensitivity of different cell types (epicardial, midmyocardial, and endocardial) to EAD development. **Methods:** Simulations were conducted using the Luo–Rudy (LRd) model of the mammalian ventricular action potential (AP). Three cell types – epicardial, midmyocardial (M), and endocardial – are represented by altering the channel density of the slow delayed rectifier current, I_{Ks}. LQTS is modelled by enhanced late sodium current (LQT3), or reduced density of functional channels that conduct I_{Kr} (LQT2) and I_{Ks} (LQT1). The cell is paced 40 times at a constant Basic Cycle Length (BCL) of 500 ms. Following a 1500 ms pause, an additional single stimulus is applied. **Results:** Our results demonstrate that pause-induced EADs develop preferentially in M cells under conditions of prolonged repolarization. These EADs develop at plateau potentials ('plateau EADs'). Mechanistic investigation shows that prolongation of the plateau phase of the post-pause AP due to a smaller delayed rectifier potassium current, I_{Ks}, and enhancement of the sodium-calcium exchange current, I_{NaCa}, allows for the reactivation of the L-type calcium current, $I_{Ca(L)}$, which depolarizes the membrane to generate the EAD. **Conclusions:** APD is a very important determinant of arrhythmogenesis and its prolongation, either due to acquired or congenital LQTS, can result in the appearance of EADs. The formation of pause-induced EADs preferentially in M cells suggests a possible role for these cells in the generation of arrhythmias that are associated with abnormalities of repolarization (e.g., TdP). The ionic mechanism of pause-induced EADs involves reactivation of the L-type calcium current during the prolonged plateau of the post-pause AP.

Keywords: Arrhythmia (mechanisms); Ion channels; Computer modelling; Long QT Syndrome; Na/Ca-exchanger

1. Introduction

The long QT syndrome (LQTS) is a cardiac disorder characterized by marked prolongation of the QT interval. It often manifests clinically as syncope, seizures, or sudden death from ventricular tachyarrhythmias, specifically torsade de pointes (TdP). To date four LQT genes have been identified and cloned [1–3]: KvLQT1 (LQT1) on chromosome 11, HERG (LQT2) on chromosome 7, SCN5A (LQT3) on chromosome 3, and MinK (LQT5) on chromosome 21. These genes encode ion-channels that play a major role during depolarization and repolarization of the action potential (AP). SCN5A encodes the cardiac sodium channel. Its mutation in LQT3 leads to impaired inactivation of sodium channels and, as a result, to a persistent component of the depolarizing I_{Na} current. An exception to this is a recently characterized mutation [4] that results in defective α–β_1 interaction. This point mutation causes a

*Corresponding author. Tel.: +1-216-368-4051; fax: +1-216-368-4969.

E-mail address: yxr@po.cwru.edu (Y. Rudy)

Time for primary review 21 days.

0008-6363/99/$ – see front matter
PII: S0008-6363(99)00035-8

shift in the voltage dependence of I_{Na} steady-state inactivation without the development of a persistent current. HERG encodes the fast cardiac delayed rectifier potassium channel. Its mutation in LQT2 acts through a dominant-negative mechanism to cause loss of function of channels that conduct I_{Kr} current. KvLQT1 is also a cardiac potassium channel that interacts with MinK to form a slow cardiac delayed rectifier potassium channel. Mutations in KvLQT1 and MinK also act through a dominant negative mechanism, causing a loss of I_{Ks} function. It follows that prolongation of repolarization and of the action potential duration (APD) are common to the diverse genetic defects, either due to loss of function of a repolarizing current (as in LQT1, LQT2, and LQT5) or due to a gain of function of a depolarizing current (as in LQT3). Abnormal cardiac repolarization and resulting susceptibility to arrhythmia can also be acquired. Agents with class III antiarrhythmic action (e.g., sotalol, dofetilide) can cause QT prolongation and TdP. Use of such class III agents results in a reduced repolarizing current and therefore, mimics the loss of function associated with HERG, KvLQT1, and MinK mutations.

The exact electrophysiological mechanism of TdP arising as a result of LQTS is still unclear, but both reentry due to dispersion of repolarization [5–9] and triggered activity associated with delayed repolarization (early afterdepolarizations) [10–14] have been proposed to be responsible for the induction and maintenance of the polymorphic arrhythmia. Early afterdepolarizations (EADs) are secondary depolarizations occurring during the course of the AP. Their appearance depends strongly on the action potential duration (APD). Prolonged repolarization, either acquired (e.g., in response to agents with class III antiarrhythmic action) or congenital (e.g., in the different types of LQTS) can result in the appearance of EADs which are associated with triggered activity and arrhythmias.

An extensive body of experimental data [15–17] has documented heterogeneity of repolarization characteristics in normal ventricular myocytes isolated from different intramural regions. Importantly, a unique subpopulation of cells (mid-myocardial M cells) has been described in guinea-pig [17], canine [16], and human [15]. These cells display a longer APD, steeper dependence of APD on rate, and a higher susceptibility to the development of arrhythmogenic EADs than other cell types in the ventricular wall. These properties suggest that the M cells might play an important role in the development of arrhythmias (e.g., TdP) that are associated with abnormalities of repolarization (for review see [18]). Studies [19] conducted in isolated canine ventricular M cell preparations show that acceleration from an initially slow rate can induce transient EADs and triggered activity via a mechanism linked to intracellular calcium loading. Other studies [20,21] have demonstrated nonuniform repolarization gradients on the epicardial surface, which under certain conditions (e.g., LQTS) can result in the development of functional conduction block and reentry, which has been proposed to play a role in the maintenance of TdP.

As stated above, the development of arrhythmias in LQTS is often associated with a pause [22–25]. In this study we investigate the effect of a pause after a period of pacing on the electrical response of isolated ventricular myocytes in the context of LQTS and the heterogeneity of cell types in the myocardium. To accomplish this goal, we use a comprehensive mathematical model of the mammalian ventricular cell (the LRd model) [26,27]. It was demonstrated [28] that the cellular heterogeneity described earlier, is associated with heterogeneity in the relative density of the two components of the delayed rectifier potassium current, I_{Ks} (slow) and I_{Kr} (rapid). In particular, M cells are characterized by a significantly lower I_{Ks} density than other cell types. Based on these results we have previously shown [29,30] that decreased I_{Ks} density results in properties that are characteristic of the midmyocardial M cells. These include prolonged APD, greater dependence of APD on rate (adaptation), and greater sensitivity to interventions that reduce repolarizing currents (e.g., agents with class III actions) or enhance depolarizing currents. Incorporating these ion channel heterogeneities and the phenotypic changes in the ionic currents associated with the different types of LQTS, we characterize the cellular response following a pause and investigate the ionic mechanism of EADs that develop under such circumstances.

2. Methods

2.1. Cell model

The theoretical dynamic model of a mammalian ventricular action potential, the LRd model [26,27], provides the basis for the simulations in this study. The model is based mostly on guinea pig experimental data; it includes membrane ionic channel currents that are formulated mathematically using the Hodgkin–Huxley approach, as well as ionic pumps and exchangers. The model also accounts for processes that regulate intracellular concentration changes of Na^+, K^+ and Ca^{2+}. Intracellular processes represented in the model include Ca^{2+} uptake and Ca^{2+} release by the sarcoplasmic reticulum (SR) as well as Ca^{2+} buffering by calmodulin and troponin (in the myoplasm) and calsequestrin (in the SR). The model also accounts [31] for the two components of the delayed rectifier potassium current, I_{Kr} and I_{Ks}.

We recently showed [29,30] that reduced density of I_{Ks} can result in electrical and pharmacological properties that are very similar to those of M cells. This behavior is consistent with previously published results by Liu et al. [28] which demonstrated a lower I_{Ks} density in M cells compared to other cell types with a uniform distribution of I_{Kr}. Therefore, the three different cell types (epicardial, M,

and endocardial) found across the ventricular wall are formulated by altering I_{Ks} density while keeping I_{Kr} constant. Heterogeneity of I_{Ks} density is introduced by altering its maximum conductance, GKs. The reader is referred to references [26,27,31] for a detailed description of the cell model and a list of equations governing the model behavior. A schematic diagram of the LRd model is shown in Fig. 1; model components are defined in the figure legend.

2.2. Simulation of acquired and congenital LQTS

Congenital LQT1 and LQT2 result from mutations in the genes encoding I_{Ks} or I_{Kr}, respectively. Evidence suggests that the electrophysiologic consequence of these mutations is a reduction in the density of functional channels. Acquired LQT results from drugs that prolong APD due to their action on multiple channels with varying degree of specificity. In our studies we reduce the maximum conductance of I_{Kr} or I_{Ks} (representing reduced channel density) to mimick acquired/congenital LQT. The use of a theoretical model enables us to study the effect of an 'ideal drug' that blocks I_{Kr} or I_{Ks} with 100% specificity. Due to this ideal specificity, such interventions can be classified as 'acquired LQT1 or LQT2'. Therefore, we refer to APD prolongation by I_{Ks} block as 'acquired LQT1' and by I_{Kr} block as 'acquired LQT2'.

Mutations in the cardiac sodium channel gene (SCN5A) result in the third form of congenital long QT syndrome (LQT3). Mutations in this gene result in a consistent phenotype: an initial rapid decay of I_{Na} (as in wild-type I_{Na}) which, unlike the wild type, is followed by a small persistent inward current due to incomplete inactivation of sodium channels. In the LRd model, which is based on the Hodgkin–Huxley scheme, the inactivation of I_{Na} is controlled by two gates, *h* (fast) and *j* (slow). To simulate LQT3, we alter the steady-state inactivation of *h* and *j* so that they do not completely inactivate. This results in a persistent late current which is 0.1% of peak I_{Na} during a voltage clamp protocol. The overall behavior of the current is in good agreement with whole cell recordings of mutant I_{Na} [32,33]. A recent study by An et al. [4] identified a novel LQT3 mutation that involves defective $\alpha-\beta_1$ interactions. This mutation affected I_{Na} through a negative shift and change in slope of the steady-state inactivation curve. Inactivation $V_{1/2}$ shifted by -16 mV while the slope changed from 7.8 to 4.9. To investigate the effects of these changes on the action potential, simulations were con-

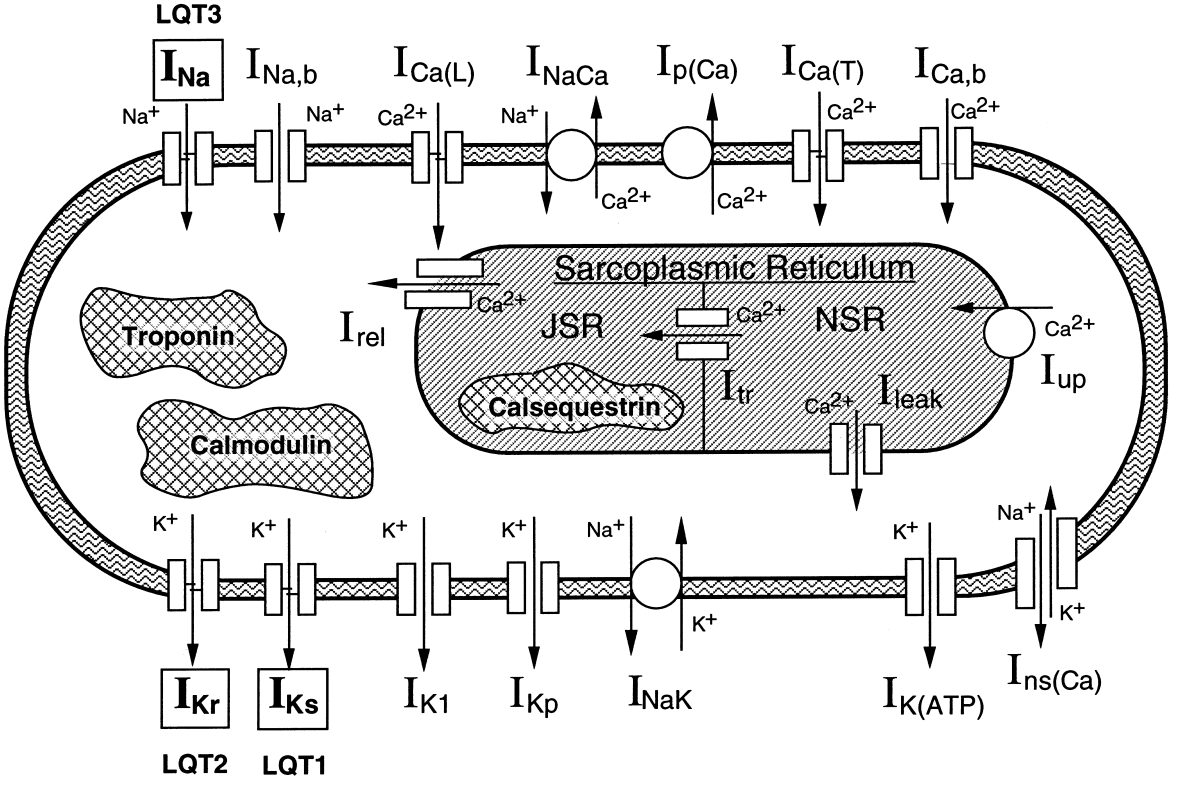

Fig. 1. Schematic diagram of the Luo–Rudy (LRd) mammalian ventricular cell model. I_{Na}, fast sodium current; $I_{Ca(L)}$, calcium current through the L-type calcium channel; $I_{Ca(T)}$, calcium current through the T-type calcium channel; I_{Kr}, fast component of the delayed rectifier potassium current; I_{Ks}, slow component of the delayed rectifier potassium current; I_{K1}, inward rectifier potassium current; I_{Kp}, plateau potassium current; $I_{K(ATP)}$, ATP sensitive potassium current; I_{NaK}, sodium–potassium pump; I_{NaCa}, sodium calcium exchange current; $I_{p(Ca)}$, calcium pump in the sarcolemma; I_{Nab}, sodium background current; I_{Cab}, calcium background current; $I_{ns(Ca)}$, nonspecific calcium activated current (activated only under conditions of calcium overload); I_{up}, calcium uptake from the myoplasm to network sarcoplasmic reticulum (NSR); I_{rel}, calcium release from the junctional sarcoplasmic reticulum (JSR); I_{leak}, calcium leakage from NSR to myoplasm; I_{tr}, calcium translocation from NSR to JSR; Calmodulin and Troponin, myoplasmic Ca^{2+} buffers; Calsequestrin, SR Ca^{2+} buffer. I_{Ks}, I_{Kr}, and I_{Na} are highlighted to indicate their participation in LQT1, LQT2, and LQT3, respectively.

ducted where the slope and $V_{1/2}$ of inactivation were similarly modified.

2.3. Simulation protocols

In the simulations, we have used a discretization time step of 1 ms during most of the AP. However, during the first 20 ms from the start of the pacing stimulus, a time step of 2 μs was used. The difference in computed APD between this adaptive protocol and a fixed time step of 2 μs is negligible, but the saving in computing time is over 30 fold per simulation. The basic protocol involved stimulation of the cell 40 times at a constant cycle length (CL) of 500 ms. After 40 stimuli, an additional stimulus (S2) was applied following a pause of 1500 ms. In order to obtain mechanistic insights, ionic currents and concentrations were computed during the course of the action potential. The strength and duration of the stimulus were 80 μA/μF and 0.5 ms, respectively. APD was measured as the interval between the time of stimulus and 90% repolarization (APD_{90}).

3. Results

3.1. Late I_{Na} (LQT3), reduced I_{Ks} (LQT1), or reduced I_{Kr} (LQT2) prolong APD

As described earlier, mutations in the SCN5A gene result in a persistent late sodium current due to incomplete inactivation of the channel. Fig. 2 shows whole cell I_{Na} currents for different (voltage clamp) test potentials computed from the 'wild-type' (WT) model (panel A) or from the 'mutant' I_{Na} model that is characterized by incomplete inactivation (panel B). The membrane is initially held at −120 mV and stepped to different voltages (−50 to 0 mV) for 200 ms. Note that peak currents are off scale at the amplification used to illustrate the late currents (the insets in panels A and B show the full scale I_{Na}). Panel C shows control (WT) I_{Na} (thin line) and 'mutant' I_{Na} with incomplete inactivation (bold line) for a single test pulse from −120 mV to −30 mV (note that the current scale is different from that in panels A and B). It is observed that incomplete inactivation of the *h* and *j* gates results in a late component of I_{Na} similar to that recorded experimentally from mutant channels [32–34], without affecting the initial rapid decay of the current from −500 μA/μF to −10 μA/μF (compare inset in panel B with inset in panel A). The persistent late I_{Na} current at −30 mV was calculated to be 0.1% of the peak current (which is within the observed values). Fig. 3 shows computed APs for control I_{Na} (thin line) and for 'mutant' I_{Na} with incomplete inactivation (bold line) in an M cell. It is observed that the late component of 'mutant' I_{Na} has a significant effect on APD despite its very small magnitude. At a BCL = 1500 ms, APD increased by 24% due to the late component of

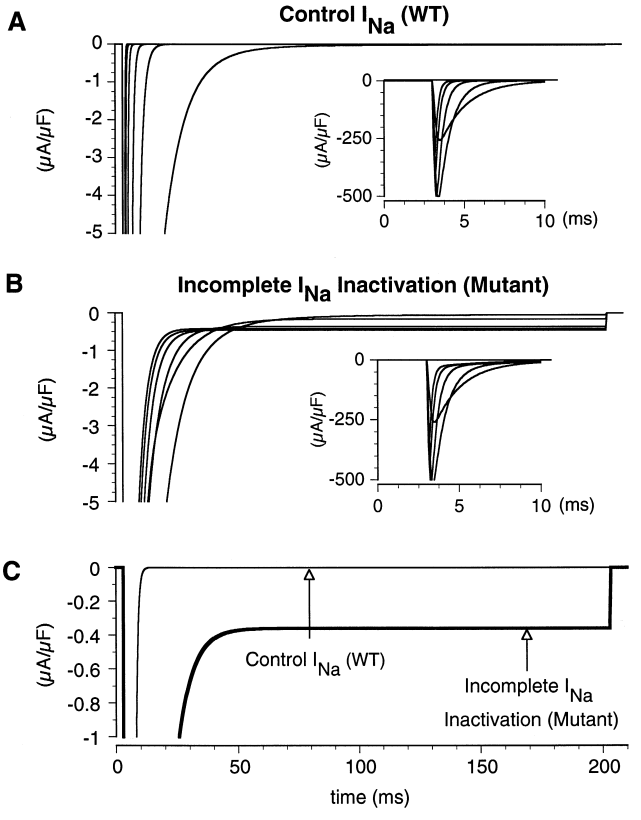

Fig. 2. Late (persistent) I_{Na} current in LQT3. The figure shows whole cell I_{Na} during voltage clamp simulated by the LRd model. Basic protocol involves the application of test pulses from a holding potential of −120 mV to different voltages (−50 to 0 mV) for 200 ms. Panel A was obtained under control conditions ('wild type', WT). Panel B was obtained during incomplete inactivation of I_{Na} ('mutant'). Note that peak I_{Na} is off scale at the magnification used to show the persistent component. Insets in panels A and B show full scale I_{Na}. Panel C shows I_{Na} on a further amplified scale for a single test potential from −120 mV to −30 mV during control (dotted line) and with incomplete inactivation (bold line). The late I_{Na} current is clearly observed in this panel.

'mutant' I_{Na}. It is also observed that the late I_{Na} increases with time. This is merely a consequence of an increase in the driving force for I_{Na} with repolarization of the membrane.

Reduced density of functional channels that conduct I_{Ks} or I_{Kr}, to simulate LQT1 or LQT2, also plays a major role in determining APD. Studies of APD changes caused by reduced I_{Ks} or I_{Kr} conductance (representing reduced channel density) have been previously conducted in our laboratory (see Fig. 4 reference [31]). The results show that APD is significantly prolonged under such circumstances.

3.2. Effect of a pause after a period of pacing

Acquired or congenital long QT syndrome is characterized by an abnormal QT prolongation and a propensity to develop into polymorphic ventricular tachycardia (torsade de pointes), and sudden death. Bradycardia or a post-

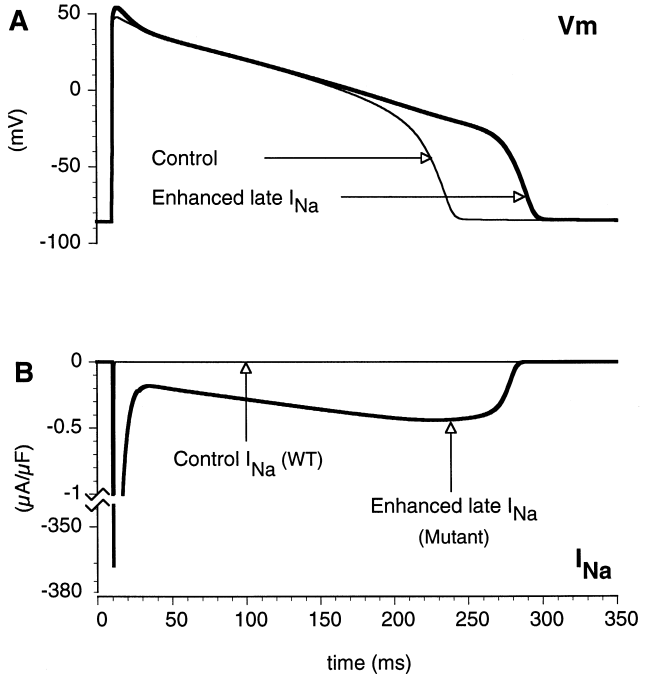

Fig. 3. Late I_{Na} in relation to the AP. Panel A shows a 'wild type' AP (thin line) and a 'mutant' AP (bold line) from an M cell. Panel B shows the corresponding I_{Na} during the AP. In the WT, I_{Na} completely inactivates and returns to zero. In contrast, in LQT3, a late non-inactivating component of the current persists which acts to prolong the AP.

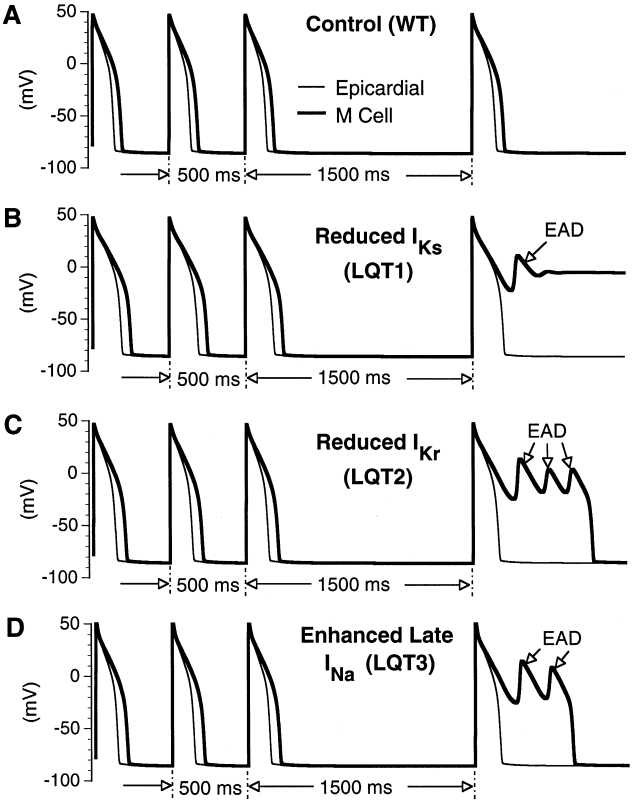

Fig. 4. Effect of pause on the development of EADs. Action potentials from epicardial and midmyocardial cells are overlayed for comparison. The figure shows the last three APs from a train of 40 APs followed by a brief pause and a post-pause AP. Under control conditions, at a BCL = 500 ms, a pause of 1500 ms results in slight APD prolongation (panel A). Under conditions of reduced I_{Ks} (LQT1, panel B), reduced I_{Kr} (LQT2, panel C) and enhanced late I_{Na} (LQT3, panel D), a pause results in the development of multiple EADs in the M cell.

ectopic pause aggravate the development of arrhythmias, probably by creating conditions that favor the development of EADs. In order to investigate the effect of a pause on EAD generation, each cell type (epicardial, M cell, and endocardial) was stimulated 40 times at a constant BCL of 500 ms. An additional stimulus (S2) was applied following a 1500 ms pause after the 40th stimulus (S1). Fig. 4 shows the last 3 APs preceding the pause and the post-pause AP. Panel A was obtained under control conditions, panel B was obtained under conditions of 70% reduction of I_{Ks} (to simulate acquired/congenital LQT1), panel C was obtained under conditions of 40% reduction of I_{Kr} (to simulate acquired/congenital LQT2), and panel D was obtained during enhanced late I_{Na} (to simulate LQT3). I_{Ks} and I_{Kr} were reduced by 70% and 40% respectively, because these were the minimum levels of reduction that resulted in pause-induced EADs. The APs from epicardial and M cell are overlaid to facilitate comparison. Data from endocardial cell is not shown as its behavior is similar to epicardial cell. It is observed from panel A that under control conditions, the pause causes slight APD prolongation of epicardial and M cells, but does not result in the development of EADs. However, reduction of either I_{Kr} or I_{Ks} or enhancement of the late I_{Na} result in the appearance of post-pause EADs with takeoff potential at -25 mV in the M cells. Under the same conditions the epicardial (thin line) or endocardial (data not shown) cells do not develop EADs. Note that in panel B the membrane potential seems to stabilize at plateau levels following the EAD; it repolarizes back to rest outside the scale shown in the figure. Shorter pause-durations (<1493 ms) failed to produce EADs even in the M cells under similar conditions of prolonged APD due to LQTS. When EADs failed to develop, the maximum APD prolongation that could be achieved was 54% (an APD change from 214 ms to 330 ms).

3.3. Effect of a pause on intracellular calcium concentrations

It is well established that pacing results in the accumulation of intracellular calcium, ($[Ca^{2+}]_i$), and the loading of Ca^{2+} into the sarcoplasmic reticulum (SR) [35]. We computed the Ca^{2+} concentrations in the junctional SR ($[Ca]_{JSR}$) and the myoplasm ($[Ca^{2+}]_i$) in an M cell. Fig. 5 panel A shows the last 5 APs from a train of 40 APs followed by a pause of 1500 ms and a post-pause AP which develops plateau EADs in the case of LQT2 (reduced I_{Kr}). The APs are shown with the computed $[Ca]_{JSR}$ (panel B) and $[Ca^{2+}]_i$ (panel C). During pacing,

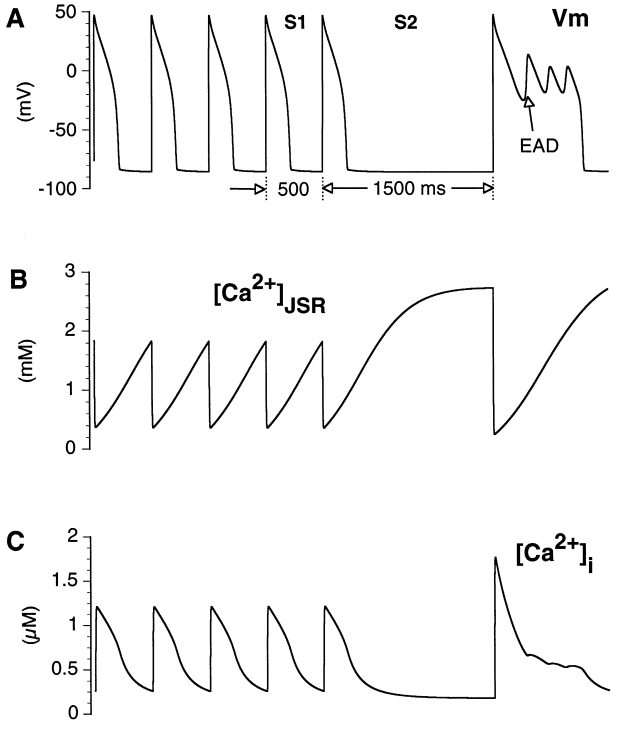

Fig. 5. Effect of pacing on intracellular calcium concentrations. Panel A: The last five APs from the train of 40 APs followed by a pause and a post-pause AP developing an EAD. Panel B: Uniform oscillation of calcium is observed in the JSR prior to the pause. During the pause there is greater build up of calcium in the JSR. Panel C: A build up of calcium in the JSR during the pause (panel B) results in a large calcium transient during the post pause AP.

calcium is loaded from the myoplasm into the network SR (NSR, loading compartment) through ATP-dependent uptake processes. The presence of a pause enables translocation of a large amount of calcium into the junctional SR (JSR, release compartment) as observed in panel B. Due to a build up of $[Ca]_{JSR}$ during the pause, a post pause stimulus elicits a large calcium release from the JSR (compared to pre-pause release) resulting in a large calcium transient (panel C). Note that this transient is almost twice the pre-pause calcium transients. The faster the prior pacing history, the greater the calcium transient during the post-pause AP.

As indicated earlier, the duration of pause plays an important role in the development of EADs. Table 1 describes the relation between pause-duration, $[Ca^{2+}]_{JSR}$, peak $[Ca^{2+}]_i$, and EAD occurrence. It is observed that for pause durations shorter than 1493 ms, EADs do not develop. With greater durations single or multiple EADs develop during the post-pause AP. It can also be seen that $[Ca^{2+}]_{JSR}$ and peak $[Ca^{2+}]_i$ increase with longer pause-durations until they reach a constant value.

3.4. Ionic mechanism of pause-induced EADs

The previous section described the effect of a pause after a period of rapid pacing on intracellular calcium concentration. To investigate the ionic mechanism responsible for the generation of the post-pause EAD, we examined selected transmembrane currents that are affected by intracellular calcium (since the major effect of the pause is to increase the intracellular calcium transient) during conditions of I_{Kr} reduction as exists during congenital or acquired LQT2. The transmembrane currents include the sodium calcium exchanger (I_{NaCa}), L-type calcium current ($I_{Ca(L)}$) that is inactivated by $[Ca^{2+}]_i$, and the slow component of the delayed rectifier potassium current, I_{Ks}, whose conductance is enhanced by $[Ca^{2+}]_i$. Based on results from Nitta et al. [35], the influence of $[Ca^{2+}]_i$ on the maximal conductance of I_{Ks} ($\bar{G}Ks$) saturates for $[Ca^{2+}]_i$ concentrations greater than 1 μM. In our simulations the peak calcium transient varies between 1 μM (pre-pause) and 2 μM (post-pause) (Fig. 5 panel C); therefore, *GKs* is affected only minimally by the pause.

Table 1
Relation between pause-duration, $[Ca^{2+}]_{JSR}$ (free Ca^{2+} in the junctional SR), peak $[Ca^{2+}]_i$ (myoplasmic free calcium transient), and EAD occurence. It can be seen that for small durations EADs do not develop. Increase of the pause duration elevates $[Ca^{2+}]_{JSR}$, peak $[Ca^{2+}]_i$, and the liklihood of EAD occurence during the post-pause AP

Pause-duration (ms)	$[Ca^{2+}]_{JSR}$ (mM)	$[Ca^{2+}]_i$ (μM)	Number of EADs
600.0	2.0795	1.395	0
800.0	2.4377	1.610	0
1000.0	2.6200	1.716	0
1400.0	2.7290	1.769	0
1493.0	2.7337	1.768	1
1497.0	2.7338	1.768	2
1500.0	2.7338	1.768	3
1600.0	2.7338	1.764	7

3.4.1. $I_{Ca(L)}$ reactivation during the long post-pause plateau generates the EAD

The inactivation of L-type calcium current involves voltage dependent and calcium dependent processes. In the LRd model they are represented by two inactivation gates, f and f_{Ca}, which are voltage and calcium dependent, respectively. The product of these two gates, $f^* f_{Ca}$, is an important parameter that indicates the recovery from inactivation of $I_{Ca(L)}$ and the availability of calcium channels for subsequent reactivation. Fig. 6, panel A shows the last pre-pause AP (thin line) and the post-pause AP (bold line) with corresponding $[Ca^{2+}]_i$ (panel B), $I_{Ca(L)}$ inactivation, $f^* f_{Ca}$ (panel C), and $I_{Ca(L)}$ (panel D). The pre- and post-pause data are overlaid to facilitate comparison. The large calcium release during the post-pause AP rapidly inactivates f_{Ca}. This rapid inactivation, observed during the initial phase of $f^* f_{Ca}$ kinetic changes (arrow in panel C), results in a smaller $I_{Ca(L)}$ during the AP plateau (panel D, black arrow). A smaller contribution

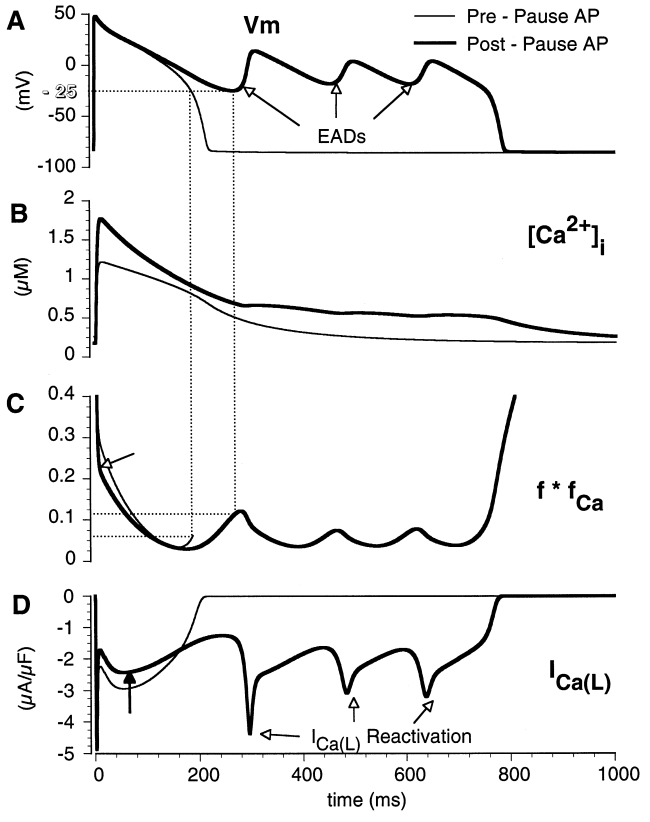

Fig. 6. Ionic mechanism of pause-induced EADs. The last pre-pause AP and a post-pause AP developing plateau EADs are shown (panel A). Also shown are corresponding $[Ca^{2+}]_i$ (panel B), $I_{Ca(L)}$ inactivation f^*f_{Ca} (panel C), and $I_{Ca(L)}$ (panel D). The arrows indicate the start of secondary membrane depolarization (EAD). The larger calcium transient during post-pause AP (panel B) results in a greater initial inactivation of $I_{Ca(L)}$ (steeper drop of f^*f_{Ca}). Panel C shows that prolongation of the plateau phase of the post-pause AP provides time for a greater degree of recovery from inactivation of $I_{Ca(L)}$ as reflected by a greater f^*f_{Ca} value. The dotted lines indicate the values of f^*f_{Ca} at the EAD takeoff potential during the pre- and post-pause AP. Greater recovery from inactivation at plateau potential during the post-pause AP allows for reactivation of $I_{Ca(L)}$ (panel D) which generates the EADs.

from $I_{Ca(L)}$ (an inward depolarizing current) actually acts to shorten APD. However, as will be shown in the following sections, this effect is more than compensated for by an enhanced inward I_{NaCa} and a smaller outward I_{Ks} during the post-pause AP. The resulting balance is a smaller outward repolarizing current during the plateau that acts to prolong APD. Prolongation of the AP plateau provides sufficient time for the recovery of the f and f_{Ca} gates from inactivation. At -25 mV (EAD takeoff potential), f^*f_{Ca} recovers to a greater extent from inactivation during the post-pause AP than the pre-pause AP (panel C, compare f^*f_{Ca} values at -25 mV, indicated by the dotted lines). The greater recovery from inactivation at a membrane potential in the range of $I_{Ca(L)}$ activation allows for the reactivation of $I_{Ca(L)}$ (panel D) which, being an inward current, results in secondary membrane depolarization to generate the EADs. When $I_{Ca(L)}$ reactivation was prevented in the simulation, EADs did not develop.

3.4.2. I_{Ks} deactivation acts to prolong the post-pause AP, allowing $I_{Ca(L)}$ to recover

It is well established that rapid pacing results in the shortening of APD (adaptation) and prevents the appearance of EADs. It has been shown [37,38] that abbreviation of APD at rapid rates involves residual accumulation of I_{Ks} activation (due to incomplete deactivation of I_{Ks} between beats) resulting in a greater repolarizing current. In this study, the M cell was stimulated 40 times at a BCL of 500 ms before the pause was applied. Presence of a pause provides more time for the deactivation of I_{Ks} before the post-pause stimulus is applied. Deactivation removes the residual accumulation of I_{Ks} activation, forcing it to activate from zero during the post-pause AP, thus resulting in a smaller repolarizing current. This is observed in Fig. 7 panel B which shows that I_{Ks} is significantly smaller during the post-pause (bold line) than the pre-pause AP

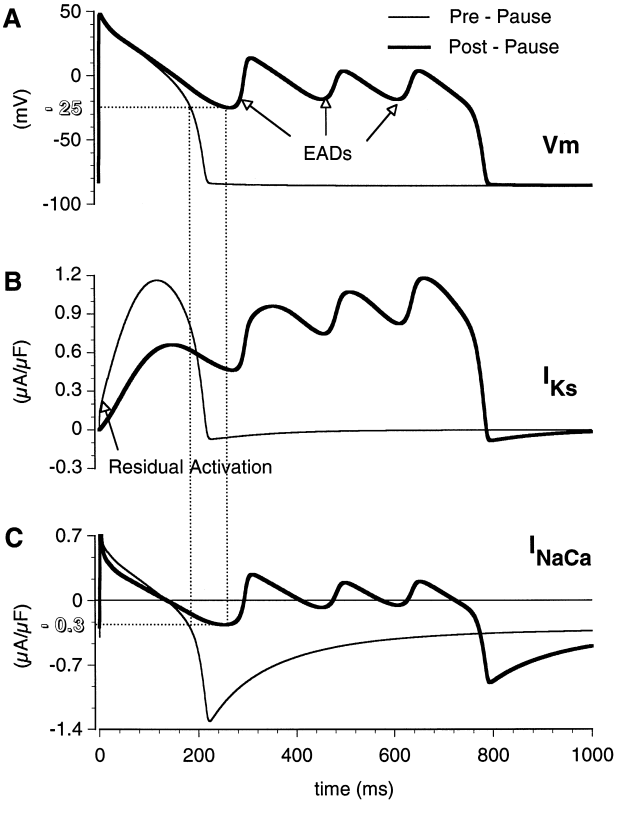

Fig. 7. Role of I_{Ks} and I_{NaCa} in pause-induced EADs. Panel A: Pre-pause (thin line) and post-pause APs (bold line) are overlayed to enable comparison in relation to I_{Ks} (panel B) and I_{NaCa} (panel C). It is observed from panel B that I_{Ks} is greater during the pre-pause AP due to residual activation at the time of stimulus application. The larger post-pause calcium transient (Fig. 5 and 6) results in I_{NaCa} becoming less outward during the early part of the AP (panel C). In combination with a smaller I_{Ks} it acts to prolong the plateau phase of the AP. The vertical dotted lines indicate the values of I_{NaCa} at the EAD takeoff potential (see text).

(thin line). A decrease in outward repolarization current results in the prolongation of the plateau phase and favors the induction of plateau EADs (panel A). To verify the role of I_{Ks} in APD prolongation simulations were conducted where complete deactivation of I_{Ks} was prevented by replacing its gate parameters just prior to the post-pause stimulus with their values just before the last AP before the pause. Fig. 8 panel A shows post-pause APs without constraints on I_{Ks} (thin line) and with imposed residual I_{Ks} activation (bold line). Imposing residual I_{Ks} activation at the outset of the post-pause AP (bold line in Fig. 8 panel B) results in a current during the AP that is similar to the pre-pause AP current (compare to thin line in Fig. 7 panel B). Under such conditions of imposed residual I_{Ks} activation (also termed I_{Ks} accumulation), the plateau phase of the post-pause AP is not prolonged and EADs do not develop (Fig. 8 panel A, bold line). Note that the more complete post-pause I_{Ks} deactivation in the unconstrained case (thin line) slows the time course of repolarization starting from the early part of the AP (arrow in Fig. 8 panel A). I_{Ks} affects the early part of the pre-pause AP despite its relatively slow kinetics because of residual activation that allows for instantaneous current to develop in response to membrane depolarization.

3.4.3. I_{NaCa} also contributes to post-pause AP prolongation, allowing $I_{Ca(L)}$ to recover

During the AP plateau, membrane potential is maintained by a very delicate balance between inward (depolarizing) and outward (repolarizing) currents. Therefore, small changes in inward/outward currents affect the APD significantly. As shown in Fig. 5, a pause following a period of pacing causes accumulation of calcium in the SR which results in a large calcium transient upon a post-pause stimulus. Fig. 7 panel C shows a pre-pause I_{NaCa} (thin line) and post-pause I_{NaCa} (bold line) overlaid to facilitate comparison. The increase in myoplasmic calcium (due to the large transient) causes I_{NaCa} to become less outward during the initial part of the post-pause AP (as it spends more time extruding calcium from the cell). This is seen by a rapid drop in the outward component of I_{NaCa} after the initial upstroke (compare bold and thin lines in Fig. 7 panel C). The reduction of outward I_{NaCa} along with a reduced I_{Ks} (Fig. 7 panel B) alters the time course and kinetics of membrane currents during the post-pause AP. This is reflected in a smaller net repolarizing current during the plateau phase of the post-pause AP. At -25 mV (EAD takeoff potential), the total repolarizing current ($I_{Kr}+I_{Ks}+I_{K1}$) during the post-pause AP is 1.1 $\mu A/\mu F$, while during pre-pause AP it is 1.5 $\mu A/\mu F$. However, the inward current due to I_{NaCa} at this potential is similar (0.25 $\mu A/\mu F$) during pre- and post- pause APs. Therefore, inward I_{NaCa} during the post-pause AP is opposed by a smaller repolarizing current, implying that the current has a greater effect in prolonging the AP. Another observation that accentuates the role of I_{NaCa} is that the time spent by the current in the inward direction until the EAD takeoff potential (-25 mV) is significantly greater during the post-pause AP than the pre-pause AP (120 ms to 40 ms), indicating a greater charge contribution to APD prolongation.

To verify the role of I_{NaCa} in EAD development we conducted simulations where I_{NaCa} was prevented from becoming inward. Fig. 8 panel C shows post-pause APs before (thin line) and after such I_{NaCa} clamp (bold line). It can be clearly seen that clamping I_{NaCa} abolishes the EADs, indicating a role for I_{NaCa} in EAD development. It can also be seen from panel C that the effect of I_{NaCa} clamp is to affect the repolarization (shortening of APD) just prior to the EAD (arrow in panel C), unlike I_{Ks} deactivation which acts to affect repolarization from the early part of the AP (arrow in panel A). It should be emphasized that I_{NaCa} does not provide the charge responsible for EAD development. It merely acts to prolong the plateau phase of the AP thereby providing time for the reactivation of $I_{Ca(L)}$ which then causes the EAD. This can be clearly seen from Fig. 7 panels A and C where it is observed that during the EAD I_{NaCa} reverses direction and becomes an outward current.

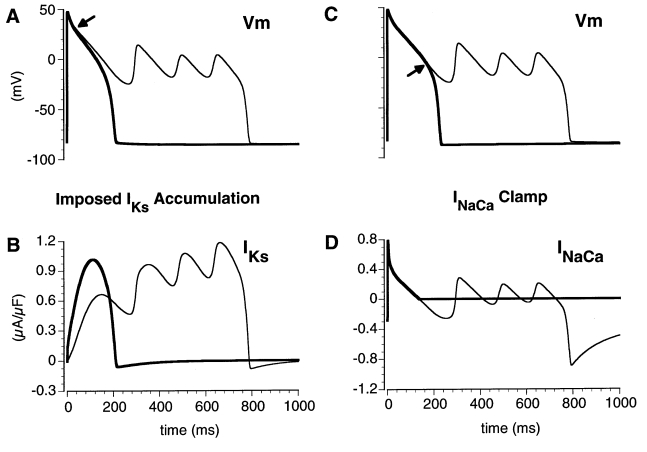

Fig. 8. Effect of imposed residual I_{Ks} activation and I_{NaCa} clamp on pause-induced EADs. Panel A: Post-pause APs before (thin line) and after (bold line) imposing residual I_{Ks} activation. Panel B: I_{Ks} before (thin line) and after (bold line) imposing residual activation. Also compare bold line in panel B with thin line in Fig. 7B. Panel C: Post-pause APs before (thin line) and after (bold line) I_{NaCa} clamp. Panel D: I_{NaCa} before (thin line) and after (bold line) it is clamped to zero prior to EAD formation. It is seen that if I_{Ks} is not allowed to completely deactivate or I_{NaCa} is not allowed to become an inward current, EADs do not develop.

4. Discussion

The study reported in this article examines the effect of a pause after a period of pacing in a mathematical model of a mammalian ventricular myocyte, under conditions of

prolonged repolarization (to simulate LQTS). Our results demonstrate that a pause can induce the development of arrhythmogenic early afterdepolarizations. The study highlights the importance of the relative density of the delayed rectifier potassium currents, I_{Ks} and I_{Kr} in the development of pause-induced EADs. Cells with decreased I_{Ks} density (e.g., midmyocardial M cells) are more prone to the development of pause-dependent EADs. The study also investigates the ionic mechanisms responsible for the development of EADs in these myocytes under conditions of imposed prolonged repolarization.

4.1. Reactivation of L-type calcium current is responsible for pause induced EADs

The slow component of the delayed rectifier potassium current, I_{Ks}, has been suggested to play an important role in rate-dependent adaptation of cardiac myocytes. At rapid heart rates, I_{Ks} accumulates due to incomplete deactivation, resulting in abbreviation of APD. The presence of a pause after a period of pacing provides time for complete deactivation of I_{Ks}. The deactivation removes residual I_{Ks} activation, resulting in a significantly smaller repolarizing current and a prolonged plateau of the post-pause AP. Another consequence of pacing is the accumulation of intracellular calcium. Apart from being a very important second messenger in various signal transduction pathways, intracellular calcium is known to play important roles in modulating different membrane ionic currents that affect the transmembrane voltage. In particular, $[Ca^{2+}]_i$ enhances the slow component of the delayed rectifier, I_{Ks}, causes inactivation of the L-type calcium current, $I_{Ca(L)}$, and drives the sodium-calcium exchanger, I_{NaCa}. Results from our simulations show a two fold increase in myoplasmic calcium upon a pause. This increase in myoplasmic calcium alters I_{NaCa} (becomes less outward) and in combination with a smaller I_{Ks}, changes the delicate balance of currents that maintain the plateau. Our studies show that interventions that affect these two currents (e.g., preventing complete deactivation of I_{Ks}, clamping of post-pause I_{NaCa}, or preventing a large post-pause calcium release) prevent the development of pause-induced EADs.

Prolongation of the post-pause AP plateau due to a smaller I_{Ks} and an enhanced inward I_{NaCa}, on the background of the LQTS effects, provides time for the recovery and reactivation of $I_{Ca(L)}$ which generates the depolarizing charge for EAD formation. When reactivation of $I_{Ca(L)}$ was prevented by clamping its value, EADs did not develop. It is important to distinguish that the primary depolarizing current responsible for the EAD generation is $I_{Ca(L)}$, while I_{NaCa} augmentation and I_{Ks} reduction merely act to prolong the post-pause plateau ('conditional phase') and set the stage for $I_{Ca(L)}$ reactivation. $I_{Ca(L)}$ reactivation seems to be a universal mechanism of EAD depolarization from plateau potentials ('plateau EADs'). However, previous studies [27,39] have shown an important role for I_{NaCa} as the main charge carrier for EAD depolarization during late phase 3 or phase 4 of the AP. The different types of LQTS also act in a non-specific manner to prolong the action potential plateau during the conditional phase. With the added pause-induced effects, prolongation of the post-pause AP due to LQT1, LQT2, or LQT3 is sufficient to cause $I_{Ca(L)}$ reactivation and EAD development. The flow chart diagram (Fig. 9) summarizes the mechanism of pause-induced EADs. It is also likely that AP prolongation, $I_{Ca(L)}$ recovery and reactivation, and EAD development may occur heterogeneously in the myocardium, thereby enhancing dispersion of repolarization and the likelihood of arrhythmias such as TdP.

4.2. LQTS and arrhythmogenesis

Torsade de Pointes, first described by Dessertenne [40], is one of the major consequences of long QT syndrome. It has been hypothesized that LQTS results in prolongation of cardiac repolarization, which predisposes the myocardium to generation of EADs. When these EADs reach a sufficient amplitude, they cause triggered activity that could be the initiating mechanism of TdP. A common feature observed and reported in several studies is a prominent pause preceding the onset of TdP (for review see [22]). Jackman et al. [23] demonstrated enhanced arrhythmia inducibility by a pause which followed a period of rapid pacing. Investigators [41] have also observed a significant increase in heart rate immediately preceding the

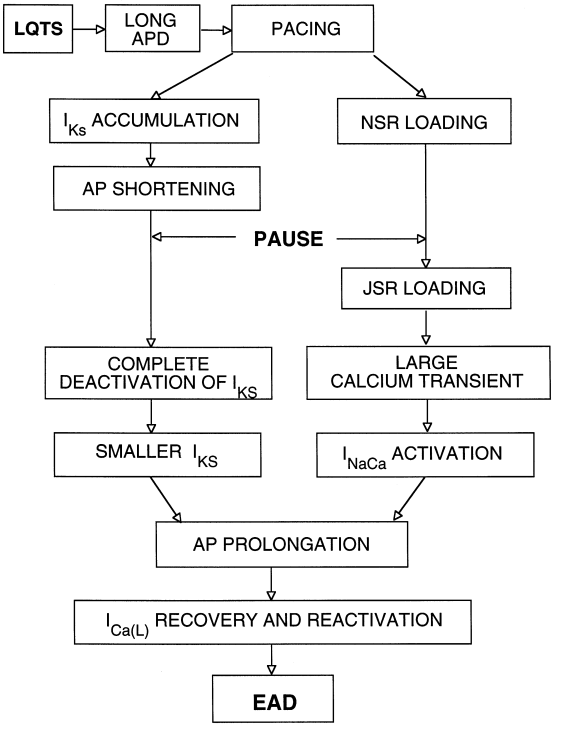

Fig. 9. Flowchart showing the sequence of events leading to the development of pause-induced EADs.

onset of arrhythmias. Leclercq et al. [24] observed prominent pauses and acceleration of the ventricular rate prior to fatal episodes of TdP and ventricular fibrillation in a large number of patients. From these studies, it becomes evident that sudden changes in cycle length favor the induction of arrhythmias. This change in cycle length has often been referred to as the short-long-short (SLS) initiating sequence and appears to play an important role in the genesis of TdP. Our studies clearly demonstrate the possibility for development of plateau EADs after a period of pacing followed by a pause, in agreement with experimental observations. We also show that development of such pause-induced EADs is dependent upon the levels of intracellular calcium and the duration of the pause. Sudden cycle length changes not only affect calcium dynamics, which in turn alters membrane ionic currents, but also has a direct effect on the kinetics of different ionic currents, in particular I_{Ks} deactivation and $I_{Ca(L)}$ recovery. The faster the initial period of pacing, the greater the role of the Na/Ca exchanger due to calcium accumulation in EAD development; the longer the pause the higher the likelihood of EAD development due to direct changes of ion channel kinetics.

The $I_{Ca(L)}$ reactivation mechanism of pause-induced EADs determined in this study is the same as that of plateau EADs generated by a variety of conditions and interventions [39,42,43]. This suggests a universal mechanism for EAD formation at plateau potentials. However, prolongation of the plateau that is necessary for $I_{Ca(L)}$ recovery and reactivation does not involve a specific mechanism. In this study we show that the pause deactivates I_{Ks} and elevates $[Ca^{2+}]_i$ to activate I_{NaCa} causing further prolongation of the plateau of an action potential that is already prolonged by LQTS. In general, any intervention that sufficiently tilts the balance of plateau currents in the inward direction can have a similar effect. Therefore, a reduction in depolarizing currents (e.g., $I_{Ca(L)}$, I_{NaCa}, or late I_{Na}) or an enhancement of repolarizing currents (e.g., I_{Kr}, I_{Ks} or $I_{K(ATP)}$) could prevent EAD development. β-adrenergic agonists increase heart rate and enhance contraction. They also exert multiple effects on cardiac cells, which include enhancement of calcium and potassium channel currents ($I_{Ca(L)}$ and I_{Ks}), increased calcium uptake by the SR, and modulation of the sodium current and the Na/K pump. We have previously shown [39] that isoproterenol (a β-adrenergic agonist) can promote the development of plateau EADs that are generated by reactivation of $I_{Ca(L)}$. In this regard, calcium channel blockers [44] and β-blockers [44,45] have been shown to reduce EAD formation and also suppress Torsade de Pointes during congenital LQTS. Shimizu et al. [46] showed a reduction in dispersion of repolarization and prevention of TdP with late sodium channel block using mexiletine. Potassium channel openers (such as nicorandil [47] that enhances $I_{K(ATP)}$) have also been shown to be very effective in the LQT1 form of congenital LQTS. A recent study [48] showed that elevation of serum potassium in patients with LQT2 resulted in reduction of the QT interval. It was suggested that this was due to the increase in the conductance of I_{Kr} (which is proportional to the square root of extracellular $[K^+]_o$). When $[K^+]_o$ was increased from 5.4 mM to 8.0 mM in our simulations of LQT2 (data not shown), pause-induced EADs were abolished. Another important observation made in this study is that the effects of a pause are less prominent with LQT1 than with the other types of LQT (note the high percentage of I_{Ks} reduction necessary to initiate pause-induced EADs in Fig. 4).

A recent study by An et al. [4] identified a novel LQT3 mutation that affects Na^+ channel activity through defective interactions between α and β_1 subunits. Specifically, they observed a shift in the voltage dependence of the steady state inactivation curve and a change in the slope factor. They did not observe any persistent late I_{Na} during whole cell measurements, in contrast to the presence of such current in other sodium channel mutations. We conducted simulations where we altered the steady state inactivation of I_{Na} as described by An et al. [4]. It was assumed in the simulations that all α subunits formed heteromeric complexes with β_1 subunits resulting in a defective $\alpha-\beta_1$ interaction, which would be the extreme case. Results suggest that the defective interaction does not affect APD significantly. It merely acts to reduce the magnitude of peak I_{Na} and to slow the time course of the initial AP upstroke. Peak I_{Na} and $(dV/dt)_{max}$ were reduced by 20% while APD *decreased* by 2 ms. Hence, the link between defective subunit interaction and prolonged repolarization during this form of LQT3 remains unclear.

Our results show that pause-induced EADs develop preferentially in M cells. The high susceptibility of M cells to APD prolongation and EAD formation suggests that they could become a source of triggered activity and focal arrhythmias, while the APD dispersion introduced by the longer APD of these cells could set the stage for the development of unidirectional block and reentry. Brugada and Wellens [49] proposed that EADs occurring at positive potentials (plateau EADs) could evoke responses from neighboring fibers that have already repolarized completely, a process they termed 'prolonged repolarization dependent reexcitation'. The presence of cells, such as the M cells, that have a greater susceptibility to the formation of pause-induced EADs than neighboring epicardial or endocardial cells could result in such a situation. Purkinje cells are similar to M cells in that they are more susceptible than other cell types to interventions that prolong APD. It is possible that EADs generated in these cells also play an important role in arrhythmias that involve prolonged repolarization and EAD formation (e.g., TdP).

4.3. Limitations of the study

The simulation studies presented here were conducted in

isolated cell models. While TdP occurs in the whole heart, characterization of the single cell behavior and its underlying ionic mechanism in isolation provides indispensable insight into the basis of its behavior in the multicellular tissue. Understanding the phenomenon at the single cell level is a prerequisite to its investigation at the multicellular tissue level, where complex interactions modulate the cellular behavior. In the intact myocardium, cells are interconnected through gap-junctions and are exposed to loading conditions that could have major effects on APD and the generation of EADs.

It is known that I_{Ks} decays more slowly than I_{Kr} in guinea-pig ventricular myocytes, but decays more rapidly than I_{Kr} in canine ventricular myocytes. Therefore, I_{Ks} accumulation might play a lesser role in determining the rate-dependence of APD in the canine. The present study shows that APD prolongation following a pause results from both I_{NaCa} augmentation and removal of I_{Ks} accumulation. It is possible that, in the canine, I_{NaCa} plays a dominant role in this process. This possibility is supported by a recent publication from Burashnikov et al. [19] that provides evidence for involvement of intracellular calcium loading and electrogenic Na/Ca exchange current in action potential prolongation in the canine.

It is well established that HERG and KvLQT1 in association with MinK form the two delayed rectifier potassium currents, I_{Kr} and I_{Ks}, that are most commonly found in ventricular myocytes. These channels are part of a large family of potassium channels which also includes Kv1.2, Kv1.4 and Kv2.1 (Shaker family) [50]. These other proteins are also known to form delayed rectifier potassium channels (e.g., the ultra rapid delayed rectifier, I_{Kur}), that have been characterized in rat and human ventricular myocytes. These currents are not incorporated in the guinea-pig type model used in this study. It is conceivable that mutations of these channels play a role in the congenital LQT syndrome. However, to date such mutations have not been identified. It will be of interest to investigate, in future studies, the effects of these currents on APD and how mutations (if identified) affect the cellular behavior.

Simulations of LQT1 and LQT2 involve reduction of the maximum conductance of ensemble I_{Ks} and I_{Kr}, respectively, while simulations of LQT3 involve the modulation of the inactivation parameters (h and j) of I_{Na} in the Hodgkin–Huxley (H–H) type model used in this study. H–H type models do not represent important properties associated with structure–function relationships of single ion channels. In particular, H–H formalism does not relate the ensemble current behavior to a specific state of the ion channel and does not account for coupling between different channel states (e.g., transitions to inactivated state only from the open state). Despite these limitations, the H–H model provides invaluable insights into cellular mechanisms underlying electrical excitation and arrhythmogenesis, and into the roles of different ionic currents during the action potential. It also helps to understand complex, highly interactive phenomena and relate them to membrane ionic currents (at the ensemble current level) and to dynamic changes in the intracellular ionic environment, as illustrated in this study.

In view of the fast growing knowledge base in the field of ion channel structure–function, it is important and timely to develop state specific models of ion channels and to integrate them into the cellular environment to study the cellular electrophysiologic manifestations of single channel properties. Such representation is especially important in the simulation of state-specific phenomena including structure–function modification due to mutation and the effects of drugs that bind to the channel protein only in a particular (e.g., open) state. Development of such models require extensive and thorough validation both in isolation and as part of the integrated cell environment, and is outside the scope of this study. Following an initial effort in our laboratory [51], we are currently in the process of developing and validating state-specific models of ion channels in the context of simulating the whole-cell behavior. The study reported here provides an important mechanistic link between cellular behavior and macroscopic (ensemble) membrane ionic currents in the LQT syndrome. The next obvious step (already in progress in our laboratory) is to relate these phenomena to single channel properties in a state-specific manner.

Acknowledgements

This study was supported by National Institutes of Health grants R01 HL-49054 and R37 HL-33343 (National Heart, Lung, and Blood Institute to Y.R.).

References

[1] Ackerman MJ. The long QT syndrome: Ion channel diseases of the heart. Mayo Clin Proc 1998;73:250–269.
[2] Wang Q, Chen Q, Towbin JA. Genetics, molecular mechanisms and management of long QT syndrome. Ann Med 1998;30:58–65.
[3] Vincent GM. The molecular genetics of the long QT syndrome: Genes causing fainting and sudden death. Annu Rev Med 1998;49:263–274.
[4] An RH, Wang XL, Kerem B et al. Novel LQT-3 mutation affects Na+ channel activity through interactions between α-β_1-subunits. Circ Res 1998;83:141–146.
[5] Surawicz B. Electrophysiologic substrate of torsade de pointes: Dispersion of repolarization or early afterdepolarizations. J Am Coll Cardiol 1989;14:172–184.
[6] Habbab MA, El-Sherif N. Drug-induced torsades de pointes: Role of early afterdepolarizations and dispersion of repolarization. Am J Med 1990;89:241–246.
[7] El-Sherif N, Caref EB, Yin H, Restivo M. The electrophysiological mechanism of ventricular arrhythmias in the long QT syndrome. Tridimensional mapping of activation and recovery patterns. Circ Res 1996;79:474–492.
[8] Qin D, Zhang ZH, Caref EB et al. Cellular and ionic basis of

arrhythmias in postinfarction remodeled ventricular myocardium. Circ Res 1996;79:461–473.
[9] Verduyn SC, Vos MA, van der Zande J, van der Hulst FF, Wellens HJ. Role of interventricular dispersion of repolarization in acquired torsade-de-pointes arrhythmias: reversal by magnesium. Cardiovasc Res 1997;34:453–463.
[10] Roden DM, Thompson KA, Hoffman BF, Woosley RL. Clinical features and basic mechanisms of quinidine induced arrhythmias. J Am Coll Cardiol 1986;8:73A–78A.
[11] Zhou JT, Zheng LR, Liu WY. Role of early afterdepolarization in familial long QTU syndrome and torsade de pointes. PACE 1992;15:2164–2168.
[12] Roden DM. Early afterdepolarizations and torsade de pointes: Implications for the control of cardiac arrhythmias by prolonging repolarization. Eur Heart J 1993;14(Suppl H):56–61.
[13] Vos MA, Verduyn SC, Gorgels AP, Lipcsei GC, Wellens HJJ. Reproducible induction of early afterdepolarizations and torsade de pointes arrhythmias by d-sotalol and pacing in dogs with chronic atrioventricular block. Circulation 1995;91:864–872.
[14] Zabel M, Hohnloser SH, Behrens S et al. Electrophysiologic features of torsade de pointes: Insights from a new isolated rabbit heart model. J Cardiovasc Electrophysiol 1997;8:1148–1158.
[15] Drouin E, Charpentier F, Gauthier C, Laurent K, Le Marec H. Electrophysiologic characteristics of cells spanning the left ventricular wall of human heart: Evidence for presence of M cells. J Am Coll Cardiol 1995;26:185–192.
[16] Sicouri S, Antzelevitch C. A subpopulation of cells with unique electrophysiological properties in the deep subepicardium of the canine ventricle. The M cell. Circ Res 1991;68:1729–1741.
[17] Sicouri S, Quist M, Antzelevitch C. Evidence for the presence of M cells in the guinea pig ventricle. J Cardiovasc Electrophysiol 1996;7:503–511.
[18] Antzelevitch C, Sicouri S. Clinical relevance of cardiac arrhythmias generated by afterdepolarizations. Role of M cells in the generation of U waves, triggered activity and torsade de pointes. J Am Coll Cardiol 1994;23:259–277.
[19] Burashnikov A, Antzelevitch C. Acceleration-induced action potential prolongation and early afterdepolarizations. J Cardiovasc Electrophysiol 1998;9:934–948.
[20] Laurita KR, Girouard SD, Rosenbaum DS. Modulation of ventricular repolarization by a premature stimulus: Role of epicardial dispersion of repolarization kinetics demonstrated by optical mapping of the intact guinea pig heart. Circ Res 1996;79:493–503.
[21] Restivo M, Caref EB, Choi B-R, Salama G. Bradycardia dependent non-uniform repolarization gradients in a guinea-pig model of long QT syndrome (LQTS)(Abstract). Circulation 1997;96:I-554.
[22] Cranefield FP, Aronson RS. The long QT syndrome and Torsade de Pointes. In: Cranefield FP, Aronson RS, editors, Cardiac arrhythmias: the role of triggered activity and other mechanisms, Futura, Mount Kisco, NY, 1988, pp. 553–579.
[23] Jackman WM, Friday KJ, Anderson JL et al. The long QT syndromes: A critical review, new clinical observation and a unifying hypothesis. Prog Cardiovasc Dis 1988;31:115–172.
[24] Leclercq JF, Maison-Blanche P, Cauchemez B, Coumel P. Respective role of sympathetic tone and of cardiac pauses in the genesis of 62 cases of ventricular fibrillation recorded during holter monitoring. Eur Heart J 1988;9:1276–1283.
[25] Kay NG, Plumb VJ, Arciniegas JG, Henthorn RW, Waldo AL. Torsade de pointes: The long-short initiating sequence and other clinical features: Observations in 32 patients. J Am Coll Cardiol 1983;2:806–817.
[26] Luo CH, Rudy Y. A dynamic model of the cardiac ventricular action potential. I. Simulations of ionic currents and concentration changes. Circ Res 1994;74:1071–1096.
[27] Luo CH, Rudy Y. A dynamic model of the cardiac ventricular action potential. II. Afterdepolarizations, triggered activity, and potentiation. Circ Res 1994;74:1097–1113.
[28] Liu DW, Antzelevitch C. Characteristics of the delayed rectifier current (I_{Kr} and I_{Ks}) in canine ventricular epicardial, midmyocardial, and endocardial myocytes. A weaker I_{Ks} contributes to the longer action potential of the M cell. Circ Res 1995;76:351–365.
[29] Viswanathan PC, Rudy Y. Differential sensitivity of ventricular cell types to class III antiarrhythmic agents (Abstract). Biophys J 1997;72:A48.
[30] Viswanathan PC, Shaw RM, Rudy Y. Effects of I_{Kr} and I_{Ks} heterogeneity on action potential duration and its rate-dependence: A simulation study. Circulation 1999:in press.
[31] Zeng J, Laurita KR, Rosenbaum DS, Rudy Y. Two components of the delayed rectifier K^+ current in ventricular myocytes of the guinea pig type. Theoretical formulation and their role in repolarization. Circ Res 1995;77:140–152.
[32] Bennett PB, Yazawa K, Makita N, George Jr. AL. Molecular mechanism for an inherited cardiac arrhythmia. Nature 1995;376:683–685.
[33] Chandra R, Starmer F, Grant AO. Multiple effects of KPQ deletion mutation on gating of human cardiac Na^+ channels expressed in mammalian cells. Am J Physiol 1998;274:H1643–H1654.
[34] Wang DW, Yazawa K, Makita N, George Jr. AL, Bennett PB. Pharmacological targeting of long QT mutant sodium channels. J Clin Invest 1997;99:1714–1720.
[35] Bers DM. Control of cardiac contraction by SR Ca release and sarcolemmal Ca fluxes. In: Bers DM, editor, Excitation contraction coupling and cardiac contractile force, Kluwer, Dordrecht, 1993, pp. 149–170.
[36] Nitta J, Furukawa T, Marumo F, Sawanobori T, Hiraoka M. Subcellular mechanism for Ca^{2+}-dependent enhancement of delayed rectifier K^+ current in isolated membrane patches of guinea pig ventricular myocytes. Circ Res 1994;74:96–104.
[37] Jurkiewicz NK, Sanguinetti MC. Rate-dependent prolongation of cardiac action potentials by a methanesulfonanilide class III antiarrhythmic agent. Specific block of rapidly activating delayed rectifier K^+ current by dofetilide. Circ Res 1993;72:75–83.
[38] Romey G, Attali B, Chouabe C et al. Molecular mechanism and functional significance of the Mink control of the KvLQT1 channel activity. J Biol Chem 1997;272:16713–16716.
[39] Zeng J, Rudy Y. Early afterdepolarizations in cardiac myocytes: Mechanism and rate dependence. Biophys J 1995;68:949–964.
[40] Dessertenne F. La tachycardie ventriculaire a deux foyers opposés variables. Arch Mal Coeur 1966;59:263–272.
[41] Locati EH, Maison-Blanche PM, Dejode P, Cauchemez B, Coumel P. Spontaneous sequences of onset of torsade de pointes in patients with acquired prolonged repolarization: Quantitative analysis of holter recordings. J Am Coll Cardiol 1995;25:1564–1575.
[42] Marban E, Robinson SW, Wier WG. Mechanisms of arrhythmogenic delayed and early afterdepolarizations in ferret ventricular muscle. J Clin Invest 1986;78:1185–1192.
[43] January CT, Riddle JM. Early afterdepolarizations: Mechanism of induction and block. A role for L-type Ca^{2+} current. Circ Res 1989;64:977–990.
[44] Shimizu W, Ohe T, Kurita T et al. Effects of verapamil and propranolol on early afterdepolarizations and ventricular arrhythmias induced by epinephrine in congenital long QT syndrome. J Am Coll Cardiol 1995;26:1299–1309.
[45] Eldar M, Griffin JC, Van Hare GF et al. Combined use of beta-adrenergic blocking agents and long term cardiac pacing for patients with the long QT syndrome. J Am Coll Cardiol 1992;20:830–837.
[46] Shimizu W, Antzelevitch C. Sodium channel block with mexiletine is effective in reducing dispersion of repolarization and preventing torsade de pointes in LQT2 and LQT3 models of the long QT syndrome. Circulation 1997;96:2038–2047.
[47] Shimizu W, Kurita T, Matsuo K et al. Improvement of repolarization abnormalities by a K+ channel opener in the LQT1 form of congenital long-QT syndrome. Circulation 1998;97:1581–1588.
[48] Compton SJ, Lux RL, Ramsey MR et al. Genetically defined therapy

of inherited long-QT syndrome: Correction of abnormal repolarization by potassium. Circulation 1996;94:1018–1022.
[49] Brugada P, Wellens HJJ. Early afterdepolarizations: Role in conduction block, 'prolonged repolarization-dependent reexcitation,' and tachyarrhythmias in the human heart. PACE 1985;8:889–896.
[50] Deal KK, England SK, Tamkun MM. Molecular physiology of cardiac potassium channels. Physiol Rev 1996;76:49–67.
[51] Zeng J. A dynamic model of a cardiac ventricular action potential. Cleveland: Case Western Reserve University, 1997 (Thesis).